

Tribological Behavior of Plant Oil-Based Extreme Pressure Lubricant Additive in Water-Ethylene Glycol Liquid

Haiyang Ding¹, Xiaohua Yang¹, Lina Xu¹, Mei Li¹, Shouhai Li¹ and Jianling Xia^{1,*}

¹Institute of Chemical Industry of Forest Products, Nanjing, 210042, China; Key Laboratory of Biomass Energy and Material, Nanjing, China; National Engineering Laboratory for Biomass Chemical Utilization, Nanjing, 210042, China; Key and Open Laboratory on Forest Chemical Engineering, SFA, Nanjing, 210042, China; Co-Innovation Center of Efficient Processing and Utilization of Forest Resources, Nanjing Forestry University, Nanjing, 210042, China.

*Corresponding Author: Jianling Xia. Email: xiajianling@126.com.

Abstract: A water-soluble lubricant additive (RSOPE) was prepared by esterification reaction using fatty acid from rubber seed oil. The RSOPE was added into water-ethylene glycol (W-EG) solution as lubricant additive. Dispersion stability and rheological properties were investigated. We used a four-ball tribotester to assess the lubrication performance of W-EG based fluid with the RSOPE additive. The stainless-steel surface was analyzed using scanning electron microscopy (SEM) and X-ray photoelectron spectroscopy (XPS). Good dispersion stability was observed in the RSOPE/W-EG solutions. Furthermore, non-Newtonian fluid behavior at low shear rates and Newtonian fluid behavior at high shear rates was exhibited. The addition of RSOPE into water-glycol reduced the friction coefficients (COF) and wear scar diameters (WSD). The maximum non-seizure loads (PB) increased from 98 N to 752 N and the W-EG solution with RSOPE had good corrosion resistance properties. Good tribological performances for W-EG solution with RSOPE were attributed to the boundary tribofilm composed of iron oxide, iron phosphide and so on.

Keywords: Rubber seed oil; fatty acid; water-soluble additive; tribological performance; friction mechanism

1 Introduction

Water-based lubricants are widely used as the metalworking fluids with high fire-resistance, good storage stability, excellent cooling abilities, and low-cost [1-3]. In practical applications, ethylene glycol is usually mixed with water, which can increase the viscosity and lubricity of water, and decrease its freezing point. Therefore, ethylene glycol can be used as lubricating base oil, and has a wide range of development and application space. Phosphorus is a commonly used active element, which has good extreme pressure and anti-wear properties in lubricating oil. Compared with sulfur element, phosphorus element has better anti-wear properties. Domestic and foreign scholars have done a lot of research on this type of additive. Luo et al. [4] studied the tribological performance of nonylphenol polyoxyethylene ether phosphate ester (PPE) solution in water-based lubricant. While PPE solutions decreased the friction coefficient to 0.15 and reduced the wear volume of by up to 50%. When the concentration was more than 0.5 wt%, PPE solution can meet the requirements of lubricating and antiwear properties. Ren et al. [5] studied a P-N type ionic liquid (T672) in synthetic ester (pentaerythritol tetraoleate known as PETO) and water-based emulsion. The results showed that the improvement of tribological properties is determined by oligomeric phosphate. W-EG-based lubricating oil still have limitations compared with the traditional petroleum based lubricating oil. These limitations include low viscosity and extreme pressure properties (maximum nonseizure load value) [6]. Thus, lubricant additives are needed to match the promise of water based lubricants.

A great deal of research has been done to enhance the lubrication properties of W-EG based lubricants. Additives can be used with W-EG based lubricants to reduce friction and wear. Many studies have

examined lubricant additives for water-glycol based lubricants. Wu et al. [7] prepared three triazine compounds for use as water-soluble lubricant additives in W-EG. The results indicated that these compounds enhanced the extreme pressure capacity and anti-wear capabilities of W-EG. Wang and others [8] synthesized Ibuprofen-based halogen-free ionic liquids (ILs) as water-based additives in water-glycol. The results showed that the friction performance of ILS is better than that of the commercial lubricant additive of Hostagloss L4 in the Wang study. As water additives, the Ibuprofen-based ILs exhibited no corrosive attacks on steel or cast iron and had extremely good hydrolytic stability in W-EG. Xiong et al. [9] prepared some N-containing heterocyclic imidazoline derivatives and used as water-soluble lubricant additives in W-EG. These improved the anti-corrosion, P_B , and friction performances of W-EG solutions. The P_B values increased by 4.7 and 6.1 times compared with W-EG fluid. Up to now, the preparation and application of bio-based and water-based in W-EG have seldom been studied. All the above lubricating additives increase the extreme pressure and wear resistance performance of the W-EG solution. However, the lubricant additives are prepared by petrochemical resources with poor biodegradability and great harm for human environment. Therefore, environmentally friendly, vegetable oil-based lubricant additives have attracted attention recently.

Vegetable oil is a clean, abundant, biomass resource. It has superior biodegradability, antioxidant stability, and wide source, low cost and mature refining technology. The main component of vegetable oil is glyceride of fatty acids, double bond and allylic carbon atom in the molecular structure of vegetable oil are susceptible to be attacked and modified for extreme-pressure and lubricating additives in water [10,11].

In this study, a new lubricant additive (RSOPE) for use in water-based lubricants was synthesized. The additive is rubber seed oil-based. The synthesized RSOPE improved the P_B values, anti-wear, and frictional properties of W-EG. The RSOPE additives also had good dispersion stability and anti-corrosion properties for copper. The friction mechanism of RSOPE in W-EG was discussed in relation to analysis the worn scar by means of SEM and XPS.

2. Experiment

2.1 Materials

Rubber seed oil (RSO) was supplied by Southwest Forestry University (Yunnan, China). Glycidol, ethylene glycol, benzyl triethylammonium chloride (TEBA), triethylamine, diethylene glycol monobutyl ether, tetrahydrofuran (THF) were obtained from Shanghai Aladdin Biochemical Technology Co., Ltd (Shanghai, China). The phenyl dichlorophosphate (PDCP) was obtained from Xuchang Huizhong fine chemical Co., Ltd (Xuchang, China).

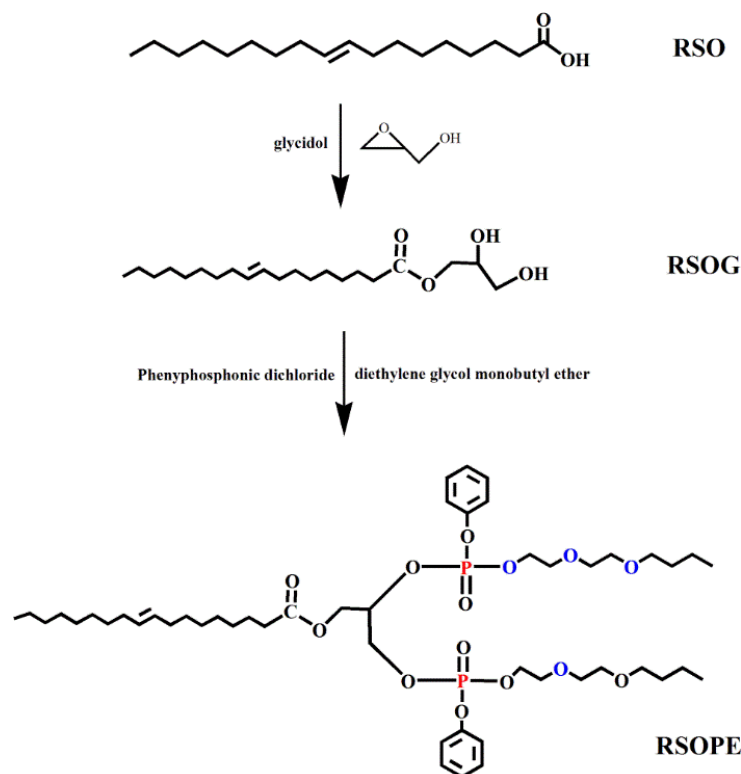
2.2 Preparation of RSO-based Phosphate Ester (RSOPE)

2.2.1 Preparation of RSO Glycidyl Ester (RSOG)

8.46 g RSO, 2.22 g glycidol, and 0.064 g (0.6 wt% of RSO and glycidol) TEBA were introduced into a fournecked flask with a mechanical stirrer, a dip tube for N_2 purge, and a thermometer. Then the mixture was heated to 120-125°C and reacted for 3 h, the RSO glycidyl ester (RSOG) was obtained.

2.2.2 Preparation of RSO-based Phosphate Ester (RSOPE)

Then 8.40 g PDCP and 40 mL THF was added into a three-necked flask, the mixture was stirred and maintained the temperature at 5°C. 8.18 g triethylamine was dropped into the PDCP solution for 30 min under N_2 atmosphere. Then a solution of 7.12 g RSOG and 30 mL THF was slowly dropped into the flask for 30 min, the solution was stirred at 25°C for 12 h. Finally, 6.48 g diethylene glycol monobutyl ether and 20 mL of dried THF was slowly dropped into the above flask and stirred at 30°C for another 12 h, then filtered and rotary evaporated. The RSO-based phosphate ester (RSOPE) was obtained (Scheme 1).



Scheme 1: Synthesis route and structure of RSOG and RSOPE

2.3 Structure Characterization

The chemical structure of RSOG and RSOPE were characterized using an IS10 FTIR spectrometer (Thermo Fisher Nicolet, USA) and an AVANCE 400 Bruker spectrometer (^1H NMR) with CDCl_3 as the solvent.

2.4 Rheological Characteristics Tests

The rheological properties of the RSOPE/W-EG samples (in solution; with $0\text{--}100\text{ s}^{-1}$ shear rate) were tested using a rheometer (US, TA, AR-2000) at 25°C .

2.5 Measurement of Tribology Properties

The friction, anti-wear and P_B values were examined by a four-ball tribometer (MRS-10A type, Xiamen Tianji Automation Co., Ltd., China), according to the ASTM D-2783 standard. The P_B values were measured at 1450 r/min for 10 s . Conditions of the COF and WSD tests were 1450 rpm (spindle speed), 200 N (loads) and 30 min (testing time).

2.6 Anticorrosion Properties

Anticorrosion properties were tested according to GB/T 6144-2010 (China) for RSOPE in W-EG solution. The test condition is $55 \pm 2^\circ\text{C}$ and 8 h , and then compared with the corrosion stands to evaluate the corrosion level.

2.7 SEM and XPS Analysis Worn Surfaces

The worn surface morphologies and chemical composition of the wear scars on steel surfaces lubricated with different RSOPE concentrations were examined on SEM (FEI Quanta 200) and XPS (PHI 5000 Versa Probe).

3 Results and Discussions

3.1 Characterization of RSOPE

Fig. 1 shows the FTIR spectrum analysis of RSO, RSOG, and RSOPE. The peak at 1710 cm^{-1} correspond to the carbonyl stretch vibration in the terminal carboxyl group. Compared with RSO, the new absorption peaks at 3389 cm^{-1} and 1742 cm^{-1} are assigned to the characteristic absorptions of the hydroxyl and carbonyl in the ester group, and the peak for carbonyl in the carboxyl group was not observed. The FTIR spectra of RSOPE, the characteristic absorption at 3389 cm^{-1} is the contribution of -OH disappear in RSOG. The characteristic absorption peaks of $\text{P}=\text{O}$ and $\text{P}-\text{O}-\text{C}$ are showed at 1207 cm^{-1} and $1017\text{-}930\text{ cm}^{-1}$, respectively.

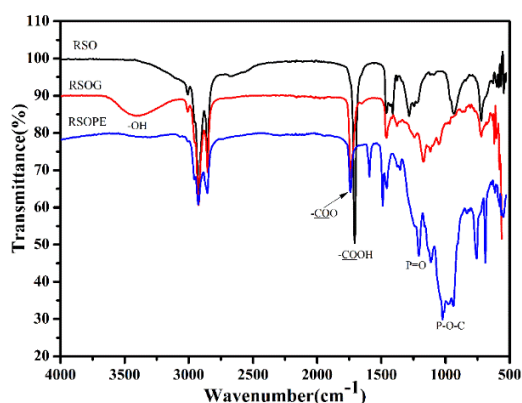


Figure 1: FTIR spectra of RSO, RSOG, and RSOPE

The $^1\text{H NMR}$ analysis results of RSO, RSOG, and RSOPE were shown in Fig. 2. $^1\text{H NMR}$ (400 MHz, DMSO), δ (ppm) = 2.78 ($-\text{CH}_2\text{-COOH}$), δ (ppm) = 11.64 ($-\text{COOH}$), δ (ppm) = 2.78 ($-\text{CH}_2\text{-COOH}$), δ (ppm) = 5.36 ($-\text{CH}=\text{CH}-$). δ (ppm) = 3.43-4.25 ($-\text{CH}_2\text{CH}(\text{OH})\text{CH}_2\text{OH}$), δ (ppm) = 2.01 ($-\text{OH}$). δ (ppm) = 6.50-7.50 (benzene-H), δ (ppm) = 3.30-3.70 ($-\text{CH}_2\text{-O}-$).

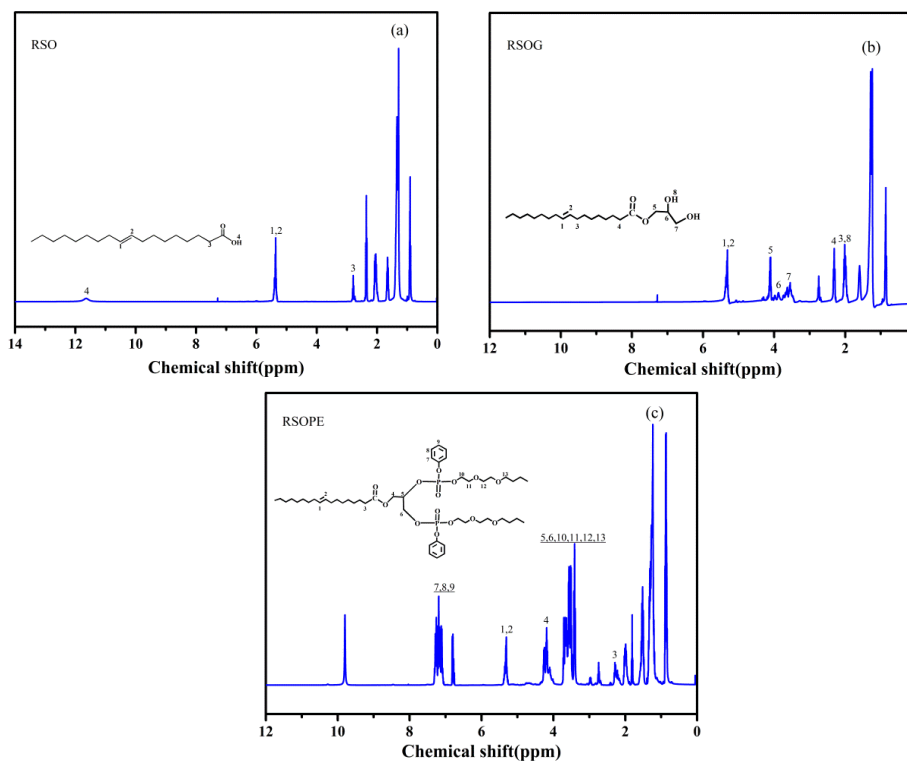


Figure 2: $^1\text{H NMR}$ spectra of RSO, RSOG, and RSOPE

3.2 Dispersion Stability

To determine dispersion stability, various concentrations of RSOPE were added to W-EG (see photos, Fig. 3). After 30 days, we found that when the concentration was less than 2.0%, the RSOPE remained well dispersed in W-EG with no stratification at the bottom of the bottles; when the concentration was 3.0%, the solution appeared to be stratified. This indicated that appropriate concentration of RSOPE had good dispersion stability in W-EG and can be used as a water-based additive in tribological applications [12,13].

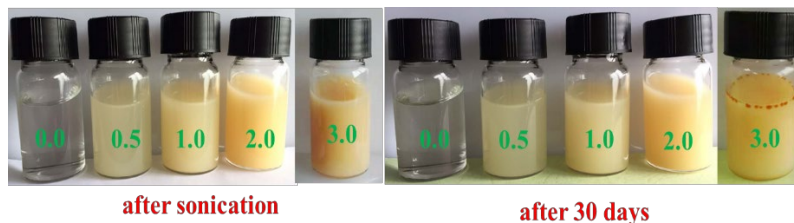


Figure 3: Digital images of W-EG based lubricants with RSOPE with concentrations ranging from 0.0 to 3.0 wt%

3.3 Rheological Characteristics

The rheological behavior of the RSOPE/W-EG solutions was investigated experimentally at 25°C at shear rates of 0 s⁻¹ to 100 s⁻¹. The varieties of viscosity and shear stress to shear rate were discussed (Figs. 4 (a)-4(b)). The results reveal that shear-thinning behavior occurred when the shear rate dropped below 20 s⁻¹. Furthermore, non-Newtonian fluid behavior was observed in solutions with lower shear rates. This is because the viscosity of RSOPE/W-EG solutions varies nonlinearly by shear rate. The shear thinning effect, however, decreased when the shear rate was above 20 s⁻¹. The viscosity of the RSOPE/W-EG solutions kepted constant and a linear relationship between the shear rate and shear stress. The RSOPE/W-EG solutions with shear rates greater than 20 s⁻¹ can, therefore, be signified the Newtonian fluid behavior [14-16].

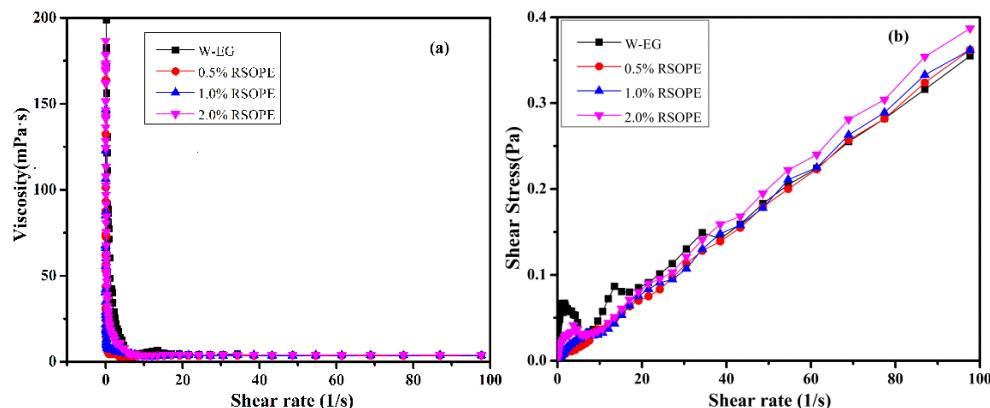


Figure 4: (a) Viscosity and (b) Shear stress as a function of shear rate for different RSOPE/W-EG solutions at 25°C

3.4 Corrosion Resistance Properties

The copper corrosion properties of RSOPE in W-EG are shown in Fig. 5 and Tab. 1. We can observe that all the RSOPE/W-EG solutions have anticorrosion properties for the copper surface and the corrosion grade were assigned as 1b. The copper strips immersed in RSOPE/W-EG solutions were no obvious corrosion and the color of the copper strips were still bright, indicating that the RSOPE additive in W-EG met the anti-corrosion requirements of WMCF for copper [17,18].

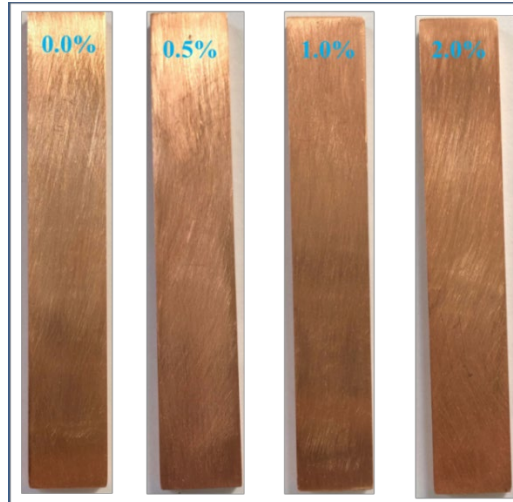


Figure 5: Copper corrosion tests of RSOPE/W-EG solutions samples

Table 1: Anticorrosion grades of test samples on copper surface

Additive	Metal	Additive concentration (%)			
		0.0	0.5	1.0	2.0
RSOPE	Copper	1b	1b	1b	1b

3.5 Extreme Pressure Properties (P_B value)

Fig. 6 shows the relationship between the concentration of RSOPE as a W-EG additive and the extreme pressure properties. The P_B value of W-EG is 98 N, indicating some difficulty in forming physical adsorption and lubrication film on the stainless-steel surface. The P_B value was improved with the addition of RSOPE; the P_B value increased with increased concentration of RSOPE. At 2.0 wt% RSOPE, the P_B value reaches 752 N, 7.7 times that of W-EG. The results contribute to the increase in the number of aliphatic chains and active phosphorus elements in RSOPE, which increases the lubricity and strengthens the loading-carrying capacity of the W-EG. This means RSOPE can produce physical adsorption and chemical reactions film on the stainless-steel surface [19-22].

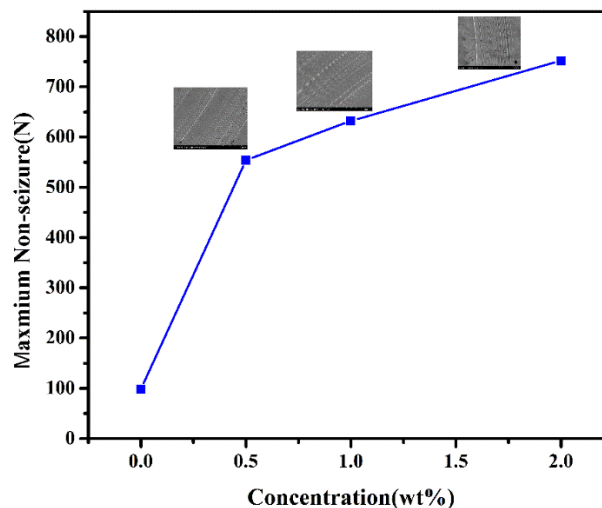


Figure 6: Effect of the RSOPE content on extreme pressure values

3.6 Antiwear and Friction-Reducing Performance

The tribological properties (COF and WSD) were tested and showed in Fig. 7. RSOPE can improved the antiwear and antifriction properties of W-EG at all concentrations. At an RSOPE concentration of 2.0 wt%, it has a COF of 0.048 and a WSD of 0.67 mm, respectively. The reason may explain as follows: Firstly, the long alkyl chains absorb on the stainless steel surface and form physical boundary lubrication film. Secondly, during the friction under high pressure, the active phosphorus in the RSOPE can react with metal and generate tribochemical reaction film [23-25].

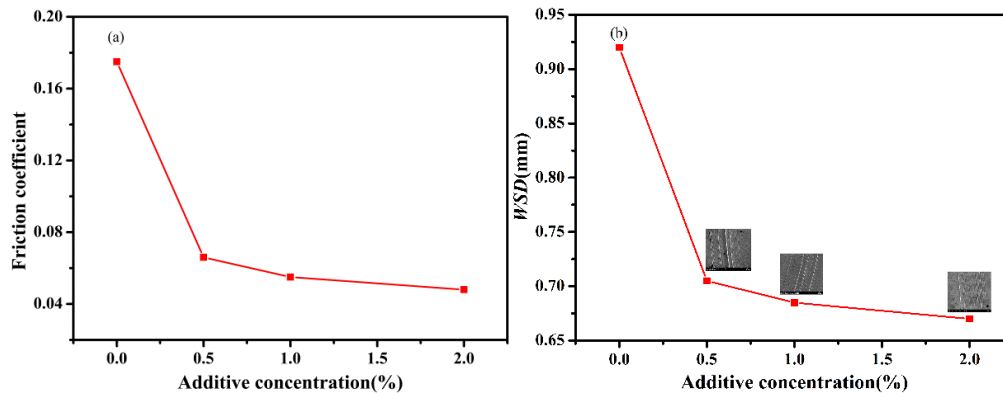


Figure 7: (a) Friction coefficient and (b) wear scar diameter at different RSOPE concentrations

Fig. 8 shows the COF of RSOPE/W-EG solutions at RSOPE concentrations of 0.0 wt%, 0.5 wt%, 1.0 wt%, 2.0 wt%. Further increasing the RSOPE concentrations, the friction coefficient of RSOPE/W-EG solutions are gradually reduced. The friction coefficient is the lowest at the same testing time when the concentration of RSOPE reaches 2.0 wt%, which indicates that RSOPE can impart good friction properties of W-EG solution. The finding confirms the results of the four-ball experiment [26,27].

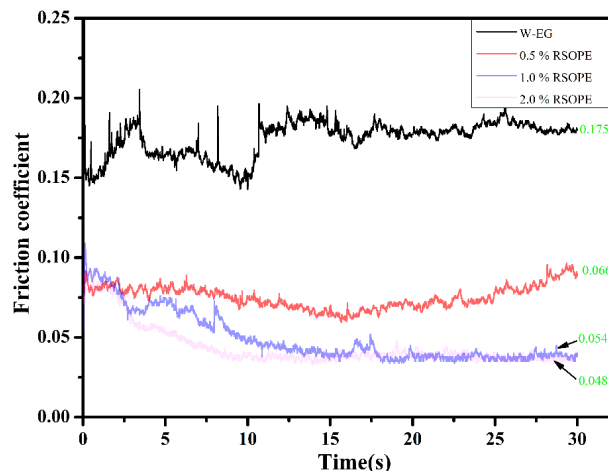


Figure 8: Influence of concentration of RSOPE on friction coefficient

Variations in COF and WSD with an applied load for W-EG and 2.0 wt% RSOPE are shown in Fig. 9. The COF values for water with 2.0 wt% RSOPE decreased with increased load. This indicates that RSOPE is more effective for improving the friction properties of W-EG under greater applied loads. With the increasing loads, however, the WSD increases. This indicates that RSOPE offers poor antiwear ability at high loads, which may be due to corrosion by phosphorus and water [28].

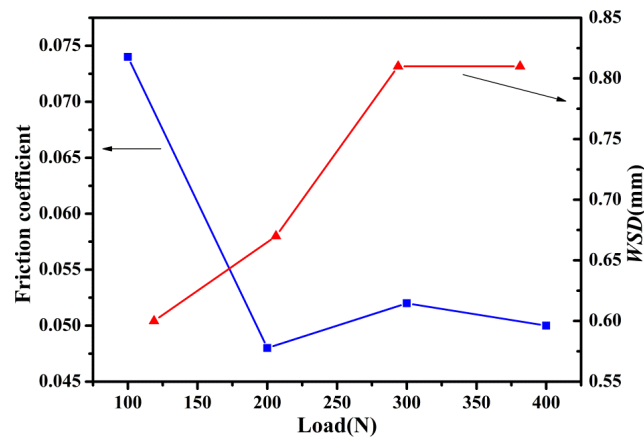


Figure 9: Influence of Load on friction coefficient and WSD

3.7 SEM Analysis

To investigate the lubricating mechanism of RSOPE, we analyzed worn steel surfaces using SEM and XPS. The SEM morphologies for stainless steel surfaces lubricated by water with different concentrations RSOPE were exhibited in Fig. 10. It can be observed that steel lubricated with small amounts of RSOPE have much wider and deeper wear scars. However, where W-EG solution and 2.0 wt% RSOPE was used as a lubricant, the surface was smooth and appeared to have a protective layer. Thus, as a water-based lubricant additive under moderate loads, the optimal additive concentration of RSOPE is 2.0 wt% [29,30].

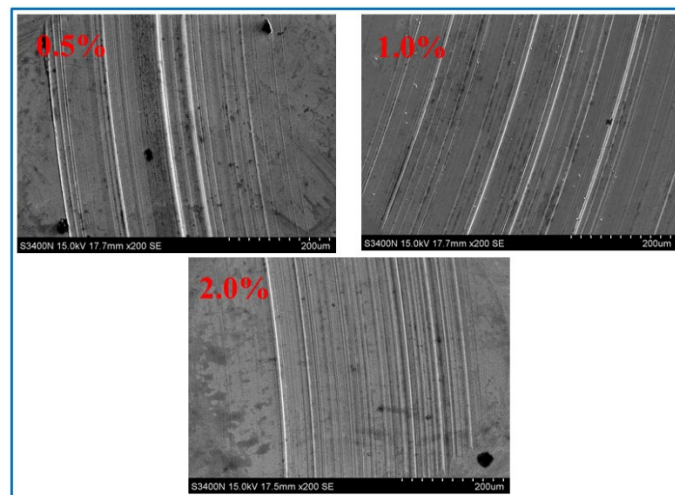


Figure 10: SEM images of the worn surfaces lubricated at different concentrations

3.8 XPS Analysis

Fig. 11 shows the XPS survey spectra of the RSOPE samples in which the characteristic C, O, P, and Fe elements are detected, and the corresponding data was shown in Tab. 2. The binding energy of 284.8 eV and 288.1 eV of C1s are assigned to the C-H, C-C, C=O and C-O bonds. This means that the RSOPE samples can form an adsorption film, which is composed of carbon and esters, etc. The XPS peaks of O1s appear at the binding energies of 529.7 eV, which may ascribed to FeO and Fe₂O₃, 530.7 eV and 531.9 eV correspond to Fe (OH)₃ and Fe₂(PO₄)₃. The peak of P2p at 133.4 eV is possibly ascribed to PO₄³⁻. The peaks of Fe2p appear at approximately 709.6 eV and 723.3 eV, which, in combination with the peak of O1s at 529.7 eV, 530.7 eV and 531.9 eV, indicates the existence of iron oxide and iron phosphate (Fe₂O₃, FeO and Fe₂(PO₄)₃) on the stainless steel surface during the friction process [31-33].

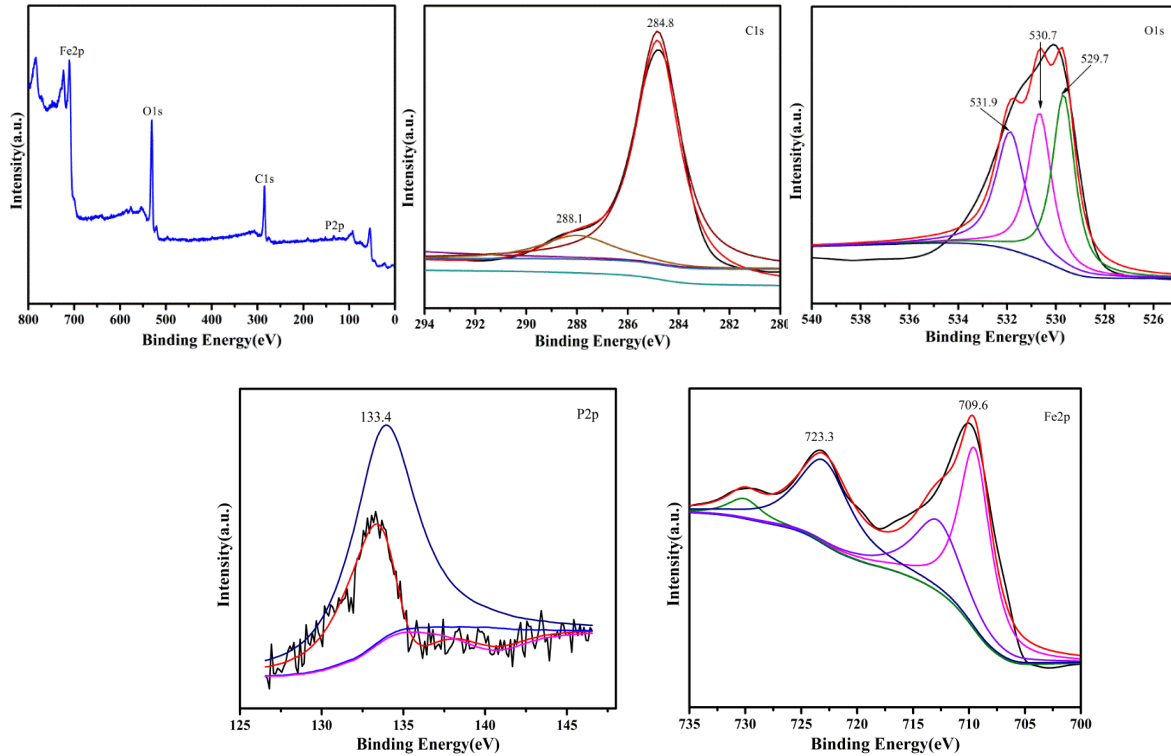


Figure 11: XPS spectra of worn surfaces lubricated with 2.0 wt% RSOPE (200 N for 30 min)

Table 2: XPS results of worn surfaces lubricated with 2.0 wt% RSOPE

Element	Binding energy(eV)	Area (%)
C1s	284.8, 288.1	41.04
O1s	529.7, 530.7, 531.9	35.85
P2p	133.4	1.13
Fe2p	709.6, 723.3	21.98

Given the above analysis, the present work finds RSOPE to be an effective lubricant additive and to improve lubrication properties due to RSOPEs ability to absorb and chemically react on metal surfaces to form boundary lubricating films of iron oxide and iron phosphate.

4 Conclusions

A new, water-based lubricant additive (RSOPE) was successfully prepared using rubber seed oil and used as an additive in W-EG. The results showed that the RSOPE/W-EG solutions had good dispersion stability. The RSOPE/W-EG solutions showed non-Newtonian fluid behavior at low shear rates and Newtonian fluid behavior at high shear rates. None of the samples corroded copper. As an additive in W-EG, RSOPE improved tribological properties. The experimental results showed that the optimal additive concentration of RSOPE was 2.0 wt%, the P_B value increased by 6.7 times (from 98 N to 752 N). The COF and WSD values reduced by 72.6% (from 0.175 to 0.048) and 27.2% (from 0.92 mm to 0.67 mm), respectively. A stable lubricating film consisting of FeO, Fe₂O₃, and Fe₂(PO₄)₃ was formed on the steel-steel contact to greatly reduce friction and wear.

Acknowledgement: This project was supported by the national key research and development program of China (Grand No. 2016YFD0600802).

References

1. Kinoshita, H., Nishina, Y., Alias, A. A., Fujii, M. (2014). Tribological properties of monolayer graphene oxide sheets as water-based lubricant additives. *Carbon*, 56, 720-723.
2. Zheng, G. L., Zhang, G. Q., Ding, T. M., Xiang, X. Z., Li, F. et al. (2017). Tribological properties and surface interaction of novel water-soluble ionic liquid in water-glycol. *Tribology International*, 116, 440-448.
3. Yan, S., Lin, B., Zhang, X. F., Wang, A. Y., Zhou, X. X. (2015). Investigation of the running-in process of silicon nitride sliding in aqueous solutions of ethylene glycol. *Tribology International*, 90, 386-392.
4. Yang, Y., Zhang, C. H., Wang, Y., Dai, Y. J., Luo, J. B. (2016). Friction and wear performance of titanium alloy against tungsten carbide lubricated with phosphate ester. *Tribology International*, 95, 27-34.
5. Zheng, G. L., Ding, T. M., Zhang, G. Q., Xiang, X. Z., Xu, Y. et al. (2017). Surface analysis of tribofilm formed by phosphorus-nitrogen (P-N) ionic liquid in synthetic ester and water-based emulsion. *Tribology International*, 115, 212-221.
6. Shahsavani, E., Afrand, M., Kalbasi, R. (2018). Experimental study on rheological behavior of water-ethylene glycol mixture in the presence of functionalized multi-walled carbon nanotubes. *Journal of Thermal Analysis and Calorimetry*, 131(2), 1177-1185.
7. Wu, Y. L., He, Z. Y., Zeng, X. Q., Ren, T. H., Vries, E. et al. (2017). Tribological and anticorrosion behaviour of novel xanthate-containing triazine derivatives in water-glycol. *Tribology International*, 110, 113-124.
8. Wang, Y. R., Yu, Q. L., Cai, M. R., Shi, L., Zhou, F. et al. (2017). Ibuprofen-based ionic liquids as additives for enhancing the lubricity and antiwear of water-ethylene glycol liquid. *Tribology Letters*, 65, 55.
9. Xiong, L. P., He, Z. Y., Han, S., Tang, J., Wu, Y. L. et al. (2016). Tribological properties study of N-containing heterocyclic imidazoline derivatives as lubricant additives in water-glycol. *Tribology International*, 104, 98-108.
10. Egbuchunam, T. O., Balköse, D., Okieimen, F. E. (2007). Effect of zinc soaps of rubber seed oil (RSO) and/or epoxidised rubber seed oil (ERSO) on the thermal stability of PVC plastigels. *Polymer Degradation and Stability*, 92(8), 1572-1582.
11. Ramadhas, A. S., Jayaraj, S., Muraleedharan, C. (2005). Biodiesel production from high FFA rubber seed oil. *Fuel*, 84(4), 335-340.
12. Song, H. J., Li, N. (2011). Frictional behavior of oxide graphene nanosheets as water-base lubricant additive. *Applied Physics A*, 105(4), 827-832.
13. Hou, K. M., Wang, J. Q., Yang, Z. G., Ma, L. M., Wang, Z. F. et al. (2017). One-pot synthesis of reduced graphene oxide/molybdenum disulfide heterostructures with intrinsic incommensurateness for enhanced lubricating properties. *Carbon*, 115, 83-94.
14. Li, P. P., Yang, R. L., Zheng, Y. P., Qu, P., Chen, L. X. (2015). Effect of polyether amine canopy structure on carbon dioxide uptake of solvent-free nanofluids based on multiwalled carbon nanotubes. *Carbon*, 95, 408-418.
15. Huang, L., Petermann, M. (2015). An experimental study on rheological behaviors of paraffin/water phase change emulsion. *International Journal of Heat and Mass Transfer*, 83, 479-486.
16. Min, T. H., Choi, H., Kim, N. H., Park, K., You, C. Y. (2017). Effects of surface treatment on magnetic carbonyl iron/polyaniline microspheres and their magnetorheological study. *Colloids and Surfaces A: Physicochemical and Engineering Aspects*, 531, 48-55.
17. Wang, J. M., Wang, J. H., Li, C. S., Zhao, G. Q., Wang, X. B. (2011). A high-performance multifunctional lubricant additive for water-glycol hydraulic fluid. *Tribology Letters*, 43(2), 235-245.
18. Wang, J. M., Wang, J. H., Li, C. S., Zhao, G. Q., Wang, X. B. (2014). A study of 2, 5-dimercapto-1, 3, 4-thiadiazole derivatives as multifunctional additives in water-based hydraulic fluid. *Industrial Lubrication and Tribology*, 66(3), 402-410.
19. Jiang, G. C., Yang, Y. Y. (2017). Preparation and tribology properties of water-soluble fullerene derivative nanoball. *Arabian Journal of Chemistry*, 10, 870-876.
20. Zhang, Y. J., Wei, L. P., Hu, H. Y., Zhao, Z. Y., Huang, Z. et al. (2018). Tribological properties of nano cellulose fatty acid esters as ecofriendly and effective lubricant additives. *Cellulose*, 25, 3091-3103.
21. Zheng, G. L., Ding, T. M., Zhang, G. Q., Xiang, X. Z., Xu, Y. et al. (2017). Surface analysis of tribofilm formed by phosphorus-nitrogen (P-N) ionic liquid in synthetic ester and water-based emulsion. *Tribology International*, 115, 212-221.

22. Dandan, M. A., Yahaya, W. M. A. W., Samion, S. (2018). The effect of fluidity of palm kernel oil with pour point depressant on coefficient of friction using fourball tribotester. *Journal of Advanced Research in Fluid Mechanics and Thermal Sciences*, 50(2), 97-107.
23. Song, H. J., Wang, Z. Q., Yang, J., Jia, X. H., Zhang, Z. Z. (2017). Facile synthesis of copper/polydopamine functionalized graphene oxide nanocomposites with enhanced tribological performance. *Chemical Engineering Journal*, 324, 51-62.
24. Wu, H., Zhao, J. W., Cheng, X. W., Xia, W. S., He, A. H. et al. (2018). Friction and wear characteristics of TiO₂ nano-additive water-based lubricant on ferritic stainless steel. *Tribology International*, 117, 24-38.
25. Dandan, M. A., Samion, S., Yahaya, W. M. A. W., Hadi, F. (2019). Tribological analysis of modified rbd palm kernel containing antioxidant additive using four-ball tribotester. *Journal of Advanced Research in Fluid Mechanics and Thermal Sciences*, 56(2), 157-164.
26. Zhang, G. Q., Xu, Y., Xiang, X. Z., Zheng, G. L., Zeng, X. Q. et al. (2018). Tribological performances of highly dispersed graphene oxide derivatives in vegetable oil. *Tribology International*, 126, 39-48.
27. Wang, Z. Q., Ren, R. R., Song, H. J., Jia, X. H. (2018). Improved tribological properties of the synthesized copper/carbon nanotube nanocomposites for rapeseed oil-based additives. *Applied Surface Science*, 428, 630-639.
28. Lei, H., Guan, W. C., Luo, J. B. (2002). Tribological behavior of fullerene-styrene sulfonic acid copolymer as water-based lubricant additive. *Wear*, 252(3-4), 345-350.
29. Pei, X. W., Hu, L. T., Liu, W. M., Hao, J. C. (2008). Synthesis of water-soluble carbon nanotubes via surface initiated redox polymerization and their tribological properties as water-based lubricant additive. *European Polymer Journal*, 44(8), 2458-2464.
30. Peng, Y. T., Hu, Y. Z., Wang, H. (2007). Tribological behaviors of surfactant-functionalized carbon nanotubes as lubricant additive in water. *Tribology Letters*, 25(3), 247-253.
31. Ma, H. B., Li, J., Chen, H., Zuo, G. Z., Yu, Y. et al. (2009). XPS and XANES characteristics of tribofilms and thermal films generated by two P-and/orS-containing additives in water-based lubricant. *Tribology International*, 42(6), 940-945.
32. Viesca, J. L., Mallad, M. T., Blanco, D., Fernández-González, A., Espina-Casado, J. et al. (2017). Lubrication performance of an ammonium cation-based ionic liquid used as an additive in a polar oil. *Tribology International*, 116, 422-430.
33. Mandrino, D., Podgornik, B. (2017). XPS investigations of tribofilms formed on CrN coatings. *Applied Surface Science*, 396, 54-559.